

| | Beer | | | GSE8894 | | | GSE3141 | | |
|---|----------|----------|-----------|----------|----------|-----------|----------|----------|-----------|
| | coef | pval | threshold | coef | pval | threshold | coef | pval | threshold |
| ASSEMBLY_OF_THE_PRE_REPLICATIVE_COMPLEX | 0.520099 | 0.000415 | 0.386737 | 1.21574 | 0.000892 | 0.861136 | 0.710268 | 0.046145 | 0.55635 |
| CYCLIN_E_ASSOCIATED_EVENTS_DURING_G1_S_TRANSITION_ | 0.42974 | 0.003513 | 0.247331 | 0.792707 | 0.027953 | 0.547786 | 0.716713 | 0.044535 | 0.213168 |
| DNA_STRAND_ELONGATION | 0.71499 | 1.00E-06 | 1.274833 | 1.071312 | 0.003607 | 1.391335 | 0.716089 | 0.04458 | 1.193017 |
| FACILITATIVE_NA_INDEPENDENT_GLUKOSE_TRANSPORTERS | 0.354506 | 0.01565 | 0.168691 | 0.763299 | 0.033131 | -0.24277 | 1.184847 | 0.001134 | -0.27284 |
| G1_S_SPECIFIC_TRANSCRIPTION | 0.830124 | 0 | 0.890295 | 0.944739 | 0.00934 | 1.179604 | 0.702067 | 0.049373 | 0.167741 |
| G2_M_CHECKPOINTS | 0.705606 | 2.00E-06 | 0.816311 | 0.904154 | 0.011586 | 1.161367 | 0.709231 | 0.04604 | 1.045875 |
| GLUCOSE_TRANSPORT | 0.770402 | 0 | 0.678839 | 0.700776 | 0.049534 | 0.284518 | 0.913949 | 0.010858 | -0.28531 |
| INTERACTIONS_OF_VPR_WITH_HOST_CELLULAR_PROTEINS | 0.545955 | 0.000228 | 0.742698 | 0.841117 | 0.019373 | 0.558675 | 0.830168 | 0.019384 | 0.185536 |
| M_G1_TRANSITION | 0.552641 | 0.000178 | 0.513903 | 1.032637 | 0.00431 | 0.877324 | 0.733152 | 0.039056 | 0.637421 |
| METABOLISM_OF_NUCLEOTIDES | 0.415754 | 0.004697 | 0.674579 | 0.987276 | 0.006085 | 0.720526 | 0.701953 | 0.048824 | 0.607988 |
| PHOSPHORYLATION_OF_THE_APC_C | 0.688238 | 3.00E-06 | 0.487527 | 0.897167 | 0.013935 | 0.775273 | 0.743429 | 0.035953 | 0.891884 |
| POL_SWITCHING | 0.765461 | 0 | 0.759954 | 1.298079 | 0.000486 | 1.169592 | 0.742413 | 0.038171 | 0.909319 |
| PROCESSING_OF_CAPPED_INTRONLESS_PRE_MRNA | 0.44213 | 0.002712 | 0.238756 | 1.199786 | 0.001042 | 0.637821 | 0.715653 | 0.043672 | 0.673775 |
| PYRIMIDINE_METABOLISM | 0.496914 | 0.000737 | 0.670047 | 0.865313 | 0.015118 | 0.505466 | 0.76726 | 0.030959 | 0.15402 |
| RECRUITMENT_OF_NUMA_TO_MITOTIC_CENTROSOMES | 0.591678 | 6.10E-05 | 0.478313 | 0.850128 | 0.01803 | 1.178261 | 0.740686 | 0.038929 | 0.960324 |
| REGULATION_OF_MITOTIC_CELL_CYCLE | 0.657655 | 9.00E-06 | 0.47527 | 0.888198 | 0.013234 | 0.760152 | 0.74365 | 0.036574 | 0.567474 |
| REPAIR_SYNTHESIS_FOR_GAP_FILLING_BY_DNA_POL_IN_TC_NER | 0.761335 | 0 | 1.102294 | 1.298079 | 0.000486 | 1.339255 | 0.906748 | 0.011015 | 1.208045 |
| SYNTHESIS_AND_INTERCONVERSION_OF_NUCLEOTIDE_DI_AND_TRIPHOSPHA | 0.495164 | 0.000785 | 0.81846 | 0.731939 | 0.040875 | 1.201097 | 0.767719 | 0.032327 | 1.280663 |
| SYNTHESIS_OF_DNA | 0.575068 | 9.80E-05 | 0.589823 | 1.032637 | 0.00431 | 0.963818 | 0.733152 | 0.039056 | 0.718498 |
| UNWINDING_OF_DNA | 0.664002 | 7.00E-06 | 1.968073 | 0.884732 | 0.013615 | 1.719352 | 0.777411 | 0.028587 | 1.531343 |

Table S1. Pathways associated with LUAD survival validated in two independent datasets logrank *P*-value, comparing tumors with the top half pathway aberrance score (Average *Z*) to the bottom.

| | Beer | | | GSE8894 | | | GSE3141 | | |
|----------------------------------|-----------|----------|-----------|-----------|----------|-----------|-----------|----------|-----------|
| | coef | pval | threshold | coef | pval | threshold | coef | pval | threshold |
| ADHERENS_JUNCTIONS_INTERACTIONS | 0.580809 | 0.003937 | 0.515289 | 0.803043 | 0.033333 | 0.478781 | 0.78677 | 0.044593 | 0.99167 |
| GAP_JUNCTION_DEGRADATION | 0.568966 | 4.55E-03 | 0.182579 | 0.831931 | 0.027237 | -0.001708 | 0.813155 | 0.037467 | -0.967199 |
| INTRINSIC_PATHWAY_FOR_APOPTOSIS | -0.472539 | 0.017116 | 0.035261 | -0.744507 | 0.044561 | 0.208941 | -0.836866 | 0.031967 | 0.165251 |
| LICAM_INTERACTIONS | 0.706449 | 0.000528 | 0.157654 | 0.88618 | 0.018241 | 0.004561 | 0.792884 | 0.037562 | 0.188119 |
| NOTCH_HLH_TRANSCRIPTION_PATHWAY | 0.390127 | 4.95E-02 | -0.141586 | 0.788812 | 0.032906 | -0.211466 | 1.097072 | 0.005562 | -0.069358 |
| PHOSPHOLIPASE_C_MEDIATED_CASCADE | 0.591627 | 0.0033 | -0.491437 | 0.928898 | 0.013105 | -0.575735 | -0.917032 | 0.01827 | -0.083575 |
| SMOOTH_MUSCLE_CONTRACTION | 0.655274 | 0.00125 | 0.437407 | 0.800452 | 0.033892 | 0.101368 | 0.937309 | 0.015528 | 0.711228 |

Table S2. Pathways associated with colon cancer survival validated in two independent datasets
logrank *P*-value, comparing tumors with the top half pathway aberrance score (Average *Z*) to the bottom.

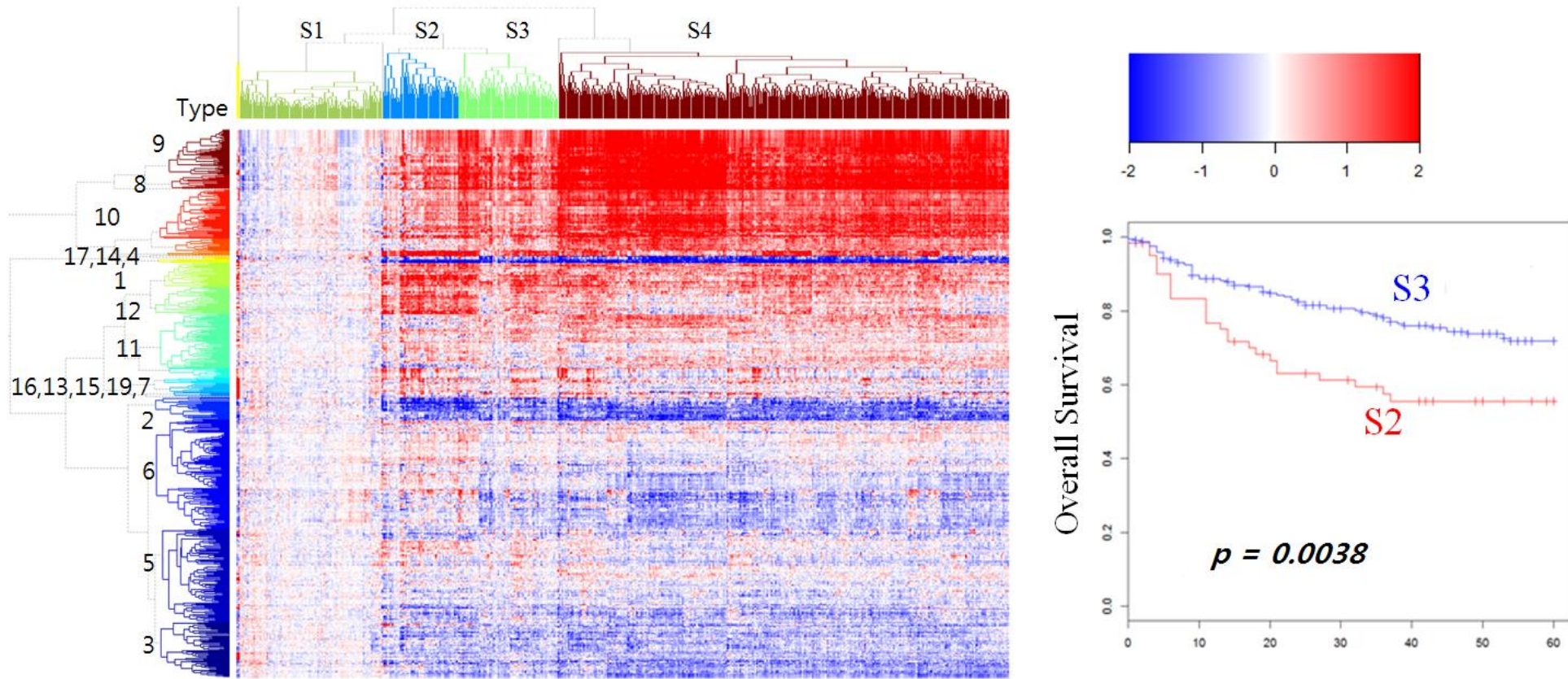


Fig. S1 Unbiased clustering using iPAS of colon cancer dataset. Pathways ($n = 583$) and samples ($n = 443$) are clustered according to iPAS (Average Z). Normal samples are clustered at left (S1). Tumors (S2–S4) deviate from normal, being both up- and down-regulated, (darker red and blue, respectively). Sample clusters represent well the overall survival of patients ($P = 0.0038$). There were no survival differences between the sample cluster pairs of (S2,S4) and (S3,S4).

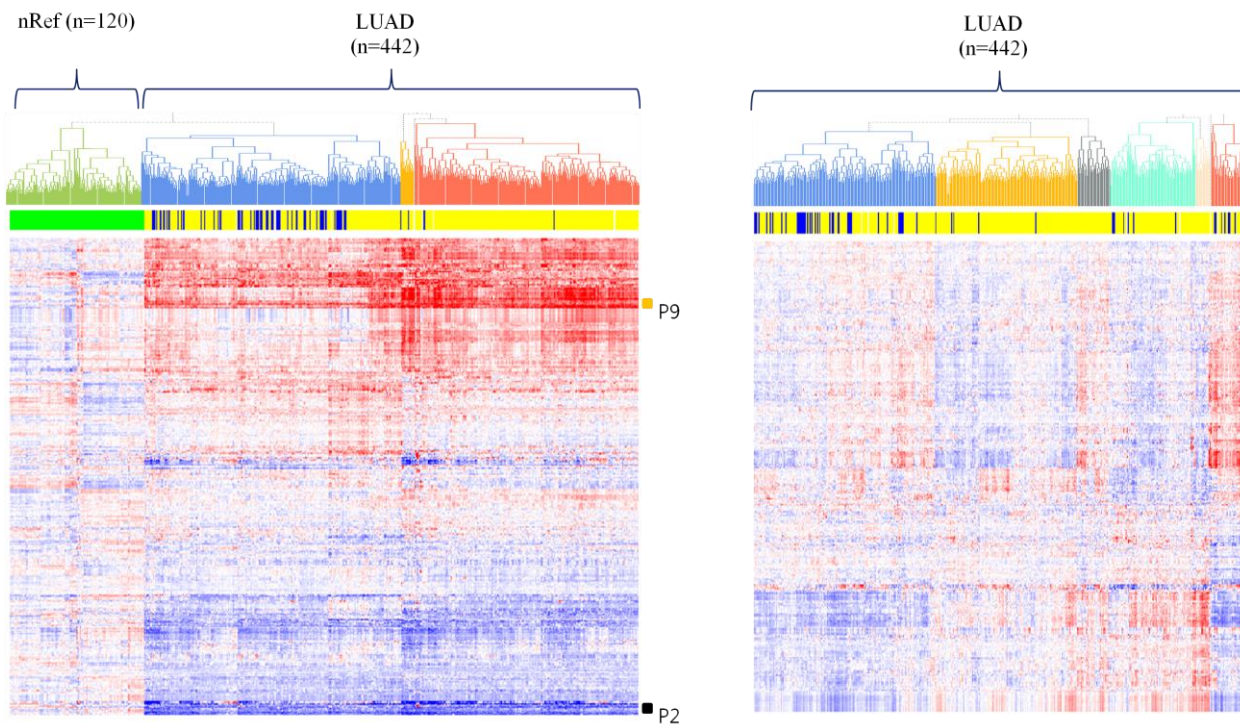


Fig. S2 nRef-based approach (left) and the conventional approach (right) provide different interpretations.

The same data was processed with two different approaches. The approach using nRef can identify globally up- or down-regulated pathways in cancer samples and can also identify variant pathways across cancer samples. The conventional approach considers all cancer samples as a cohort, and then normalizes all of the samples together. Pathway score is represented in the conventional approach by averaging standardized gene expression values, where the mean and standard deviation of all cancer samples are used for standardization. Because an individual sample's pathway statistic is affected by the context of other cancer samples, pathways commonly up- or down-regulated in all cancer samples can be obscured.

| Pathway name (REACTOME) | Average Z | GSEA | Fisher | Euclidean | Mahalanobis | Mean |
|--|-----------|-------|--------|-----------|-------------|-------|
| REACTOME_AMINO_ACID_SYNTHESIS_AND_INTERCONVERSION_TRANSAMINATION | 0.936 | 0.950 | 0.914 | 0.958 | 0.980 | 0.947 |
| REACTOME_UNWINDING_OF_DNA | 0.937 | 0.942 | 0.833 | 0.920 | 0.937 | 0.914 |
| REACTOME_O_LINKED_GLYCOSYLATION_OF_MUCINS | 0.925 | 0.939 | 0.833 | 0.955 | 0.910 | 0.912 |
| REACTOME_SYNTHESIS_AND_INTERCONVERSION_OF_NUCLEOTIDE_DI_AND_TRIPHOSPHA | 0.941 | 0.953 | 0.738 | 0.932 | 0.946 | 0.902 |
| REACTOME_APC_CDC20_MEDIATED_DEGRADATION_OF_NEK2A | 0.885 | 0.906 | 0.799 | 0.945 | 0.948 | 0.897 |
| REACTOME_PURINE_RIBONUCLEOSIDE_MONOPHOSPHATE_BIOSYNTHESIS | 0.905 | 0.915 | 0.820 | 0.921 | 0.912 | 0.895 |
| REACTOME_PURINE_METABOLISM | 0.915 | 0.918 | 0.729 | 0.945 | 0.936 | 0.889 |
| REACTOME_DNA_STRAND_ELONGATION | 0.889 | 0.920 | 0.783 | 0.930 | 0.916 | 0.888 |
| REACTOME_DEGRADATION_OF_THE_EXTRACELLULAR_MATRIX | 0.839 | 0.906 | 0.804 | 0.964 | 0.918 | 0.886 |
| REACTOME_G1_S_SPECIFIC_TRANSCRIPTION | 0.837 | 0.876 | 0.813 | 0.945 | 0.957 | 0.886 |
| REACTOME_G0_AND_EARLY_G1 | 0.873 | 0.888 | 0.767 | 0.948 | 0.948 | 0.885 |
| REACTOME_KINESINS | 0.862 | 0.878 | 0.809 | 0.928 | 0.938 | 0.883 |
| REACTOME_GLUONEOGENESIS | 0.890 | 0.910 | 0.783 | 0.903 | 0.902 | 0.877 |
| REACTOME_ACTIVATION_OF_THE_PRE_REPLICATIVE_COMPLEX | 0.892 | 0.908 | 0.737 | 0.909 | 0.918 | 0.873 |
| REACTOME_E2F_MEDIATED_REGULATION_OF_DNA_REPLICATION | 0.903 | 0.903 | 0.725 | 0.925 | 0.893 | 0.870 |
| REACTOME_DEPOSITION_OF_NEW_CENPA_CONTAINING_NUCLEOSOMES_AT_THE_CENTROM | 0.911 | 0.930 | 0.828 | 0.966 | 0.706 | 0.868 |
| REACTOME_EXTENSION_OF_TELOMERES | 0.840 | 0.889 | 0.762 | 0.913 | 0.926 | 0.866 |
| REACTOME_CELL_CYCLE | 0.894 | 0.922 | 0.766 | 0.955 | 0.780 | 0.863 |
| REACTOME_INHIBITION_OF_THE_PROTEOLYTIC_ACTIVITY_OF_APC_C_REQUIRED_FOR_ | 0.852 | 0.881 | 0.745 | 0.888 | 0.951 | 0.863 |

Table S3. AUC of pathway-based classification of tumor sample via different pathway summary methods